

## Response to Reviewer 1

We thank Reviewer 1 for her thoughtful and helpful review of our paper. The comments have helped us improve the manuscript significantly. Our reply to reviewer comprises two parts: (1) some short general statements and (2) point-by-point reply to comments from reviewer. Reviewers comments are in blue type. Extracts from our revised manuscript are in italics.

### Section one: general statements

#### *1. This work contains data which are completely new.*

We would like to emphasize that the sequence of microstructures and CPOs developed with increasing strain has not been documented before for ice deformed at cold temperatures (-20, -30 °C). This is highlighted by one of the comments by the reviewer: “The hypothesis that GBM being less active at low temperature, the impact of grain rotation driven by intracrystalline slip prevails is much clearer, especially since it is very coherent with the observations that the cone angle is reduced, and more orientations are found close to the vertical. This assertion is, indeed, justified by the experimental observations. This is, in fact, the main “novelty” of the presented work and should be emphasised more.”

Earlier work showing the up-strain microstructures and CPOs (e.g. Jacka & Macagnan, 1984; Montagnat 2015) are at warm conditions where the CPO evolves towards an open cone (small circle). Experiments at colder temperatures (-30 °C and colder) to strains of ~ 20% (Craw et al., 2018; Prior et al 2015) show CPOs have maxima of c-axes parallel to compression. No published work shows the up-strain evolution of microstructures or CPOs at -20 or -30 °C (or colder temperatures). Jacka & Li (2000) show CPOs at ~10% strain at ~ -15 and -20 °C and ~ 3% strain at -45 °C but include no microstructural data and do not explore the up-strain evolution. Recent work by Wilson et al (2019) shows CPOs at -15 and -20 °C at 20% strain, but show no up-strain evolution. In this paper the up-strain sequence at -30°C documents the evolution towards a cluster CPO, the sequence at -10 °C the evolution towards an open cone CPO and the sequence at -20 °C something between these two. Understanding how and why different CPOs develop as a function of temperature should give a better insight into the mechanisms that control CPO development and mechanical behaviour.

#### *2. Different interpretations can be made from the same observation.*

One of the reviewer’s objections relates to our interpretation of the microstructural development as involving grain boundary sliding (GBS). We accept that the factual observations could be interpreted in different ways and in the revision, we include some alternative interpretations (including “spontaneous” nucleation) of the data, with some discussion of the merits and drawbacks of each of these interpretations. We hope that we have kept the observations and interpretations clearly separated and we have reduced the emphasis on our preferred interpretation of GBS. We have also identified some of the tests that may facilitate distinguishing these different interpretations in the future. Some more details are included in answers to specific points.

The reviewer’s comments highlight that our original manuscript did not really make clear that we do interpret intracrystalline dislocation glide that causes lattice rotation as one of the key processes controlling CPO development. We hope that we have made this much clearer in the revised manuscript. The operation of a GBS process, if this is correct, would be additional to the role of intracrystalline dislocation glide and associated recovery and recrystallisation processes.

## Section two: point-by-point reply to comments

1. P3 l. 28: why should the sample be cooled in liquid nitrogen? Couldn't that induce some thermal stress due to the fast and strong temperature gradient? Changes in local microstructure, dislocation arrangements, etc. are expected to occur in the first minutes after the test... so this quenching should not avoid it.

The purpose of cooling deformed ice samples in liquid nitrogen is to preserve the ice microstructure during a long-term storage and also for intercontinental transfer (using a nitrogen dry shipper). The time interval between ice deformation work and cryo-EBSD analyses is normally longer than one month. Very cold storage has several advantages:

1. The colder temperatures minimise the chance of long-term microstructure change.
2. The storage is much more reliable than storing in an electric freezer. The dewar usually lasts one to two months between liquid nitrogen top ups and can easily stay cold for > 6 months if fully filled (as has just been done for COVID 19 lock down).
3. The storage solution is much cheaper than a very cold (-80C) freezer.

Thermal shock is a risk with liquid nitrogen storage. Plunging a -20°C sample directly into liquid nitrogen will cause the sample to shatter. More careful handling prevents any fracturing. We have some samples (e.g. MIT666 (Prior et al., 2012)) that have been cycled between liquid nitrogen and much warmer temperatures (e.g. for grain growth experiments (Becroft, 2015)) with no discernible changes to structure or microstructure. We applied a staged cool-down method to progressively cool deformed samples to a liquid nitrogen temperature:

1. Firstly, samples are cooled down to -30 °C in a chest freezer for ~5 minutes while the indium jacket is being peeled off.
2. Secondly, samples are transferred into liquid nitrogen mist at ~ -100 °C for ~10 minutes.
3. Finally, samples are transferred to a liquid nitrogen dewar for a long-term storage.

We use the staged cool-down process to prevent a drastic temperature change, which might lead to thermal stress in sample. The staged cool-down method was not clarified in the manuscript and it has been clarified in the modified version.

We always worry that there could be some post-deformational changes that change the sample microstructure after load has been removed but before the sample is “quenched”. Our procedures try to minimise this and as a minimum, ensure all samples are treated in a similar way. After each deformation run ended, we drove back the driving piston, depressurized the pressure vessel, and extracted the sample from deformation rig in 10 to 30 minutes. Each sample was exposed at room temperature for less than 30 seconds for taking photos. Soon after, the samples were cooled down to a liquid nitrogen temperature using the staged cool-down method.

Static annealing of the ice microstructure during the sample extraction is a potential issue in all ice deformation experiments. The experiments shown by Hidas and others (2017) quantified the ice microstructural changes during thermal annealing at -5 to -2 °C. They show no significant ice microstructural change in pre-deformed samples over the time scales of our sample extraction process. More specifically, Hidas and others (2017) shows deformation-induced tilt boundaries and kink bands remain stable during early stages of annealing. It takes >24 h of annealing to start to erase these microstructures.

We have added a statement into section 2.2: “*Minor static recovery of the ice microstructures may happen on this timescale (Hidas et al., 2017), but significant change in CPO or grain size is unlikely.*”

2. P7 l. 8-10: in the paragraph just before it is mentioned that the grain size distributions are mostly bimodals, and therefore not gaussians... The mean and STD parameters are therefore not suited to described them, since they do not represent well the given statistics. I therefore suggest the authors to provide medians and quartile data instead to better fit the type of distributions observed.

The reviewer has a good point and we have addressed this by including a wider range of grain size measurements, that may reflect better a scalar representation of a skewed distribution; for example, we have added median and quartile grain size values to Table 3. We have also kept the values of mean grain size in the paper, as this is a common measure used in microstructural studies and provides some comparability to those studies.

3. P7 l. 30: couldn't it exist a bias link to the lack of resolution in step size and misorientation when getting toward smaller subgrains?

We'll discuss the two issues separately:

The data filtering process removes grains with area equivalent diameters lower than 20  $\mu\text{m}$ . Thus, there is an artificial lower cut off to the grain size and sub grain distributions (as there always is for any microscopic method). Our grain size distributions show peaks above the 20  $\mu\text{m}$  cut off, these peaks are unlikely to change even though we may miss some smaller grains. The subgrain peak in all cases is  $\sim 20 \mu\text{m}$  (i.e. at th resolution cut-off), particularly at lower temperatures. The true peak subgrain size is therefore likely to be  $< 20 \mu\text{m}$  and it is probable that we are missing a substantial population of smaller subgrains in our analyses. We acknowledge this limitation and have added a statement into section 3.3.3: “*In many cases, particularly at lower temperatures, the peak corresponds to the lower grain size resolution (cut off) indicating that we could be missing smaller subgrains. For this reason, the peak subgrain sizes are not useful and the median and mean subgrain sizes probably represent overestimates.*”

The orientation resolution in these EBSD maps is  $\sim 0.5^\circ$ , so that we cannot reliably identify misorientations of  $\sim 1^\circ$ . The misorientation threshold chosen for identifying subgrain boundaries is  $\geq 2^\circ$ , the lowest angle that returns reliable results for our data. Lower angle subgrain boundaries could exist and at least one comparison of TEM and EBSD has shown that this is the case (in quartz :(Shigematsu et al., 2006)). We have added a statement into section 2.4: “*The angular resolution (error of crystallographic orientation measurement of each pixel) of the EBSD data is  $\sim 0.5^\circ$ .*”

4-1. Part 3.2.3: this is not clear to me how is the subgrain size defined and calculated.

Thanks for pointing our lack of clarity in defining how subgrain size was defined and calculated.

We have added a statement in section 2.5.1: “*Deformed ice is often characterised by a development of subgrain boundaries where the misorientations between neighbouring pixels are lower than the misorientation angle threshold of grain boundaries (e.g. Montagnat et al., 2015; Weikusat et al., 2017). An ice grain can be separated into several subgrains by one or more subgrain boundaries. We calculated subgrain size using boundary misorientation thresholds of  $\geq 2^\circ$ . Grain size and subgrain size were calculated as the diameter of a circle with the area equal to the measured area of each grain or subgrain.*”

4-2. Although we observe a clear grain boundary structure in the figures, there appears no clear subgrain structure (as one could observe in some minerals or metals for instance). On the contrary, subgrains appear more like straight tilt bands or kink bands, with, in some places, some variations around the straight shape.

We agree with the observation from the reviewer that suggests many of the subgrain boundaries are straight tilt bands or kink bands. The subgrain structure in the submitted manuscript version was revealed by the Weighted Burgers vector (WBV) method. We didn't make it clear that the measurement of subgrain sizes were not based on the WBV data, but on the misorientations between adjacent pixels. The WBV was a legacy of a much earlier manuscript and the reviewer's comments have highlighted that it is better removed. The new maps (Fig. 4(c), 5(c), 6(c)) show subgrain boundaries that correspond to the much simpler misorientation threshold. We modified statements on section 3.3.1 to: “*Distinct sub-grain boundaries can be observed in all the samples (Fig. 4 (c), 5 (c) and 6 (c)). Many of the subgrain boundaries appear to be straight, some with slight curvature. A small number have strong curvature. Interconnected subgrain boundaries can be observed in some of the grains. Subgrain boundaries subdivide grains into subgrains.*”

Figure R1.1 shows the structures of subgrain boundary in deformed ice samples as well as other experimentally or naturally deformed minerals and metals, e.g. quartz (Cross et al., 2017; Killian and Heilbronner, 2017), Olivine (Hansen et al., 2012), Magnox alloy (Wheeler, 2009) and Zircon (MacDonald et al., 2013). We added a new statement section 4.1.2: “*The subgrain boundary geometry is comparable with other experimentally or naturally deformed rock and metal samples, e.g. quartz (Cross et al., 2017a; Killian and Heilbronner, 2017), Olivine (Hansen et al., 2012), Magnox alloy (Wheeler, 2009) and Zircon (MacDonald et al., 2013).*”

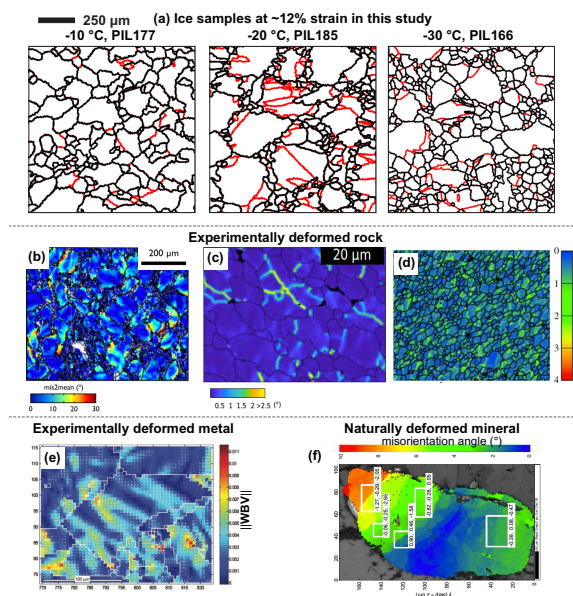


**Figure R1.1.** Illustrations of subgrain boundaries developed in experimentally deformed materials. **(a)** Experimentally deformed ice samples to ~12% true axial strain at -10, -20 and -30 °C from this study. Sub-grain boundaries where misorientation between neighbouring pixels between 2° and 10° are coloured red. Grain boundaries where misorientation between neighbouring pixels higher than 10° are coloured black **(b)** Experimentally deformed quartz sample W1051 (189±30 MPa, 1000 °C, 41% axial strain,  $1.9-2.9 \times 10^{-5} \text{ s}^{-1}$ ) from Cross et al., 2017. Each pixel is coloured by the value of mis2mean (misorientation between each pixel and the mean orientation of their parent grain). **(c)** Experimentally deformed quartzite sample W946 (1.5 GPa, 875 °C, 3.3 shear strain,  $3.1 \times 10^{-5} \text{ s}^{-1}$ ) from Killian and Heilbronner, 2017. Each pixel is coloured by Kernel average misorientation (KAM) of a 24-pixel neighbourhood. **(d)** Experimentally deformed olivine sample PT0552 (136 MPa, 8.8 shear strain,  $0.551 \times 10^{-3} \text{ s}^{-1}$ ) from Hansen et al., 2012. Each pixel is coloured by local misorientation calculated with 5 by 5 pixel averaging filter. **(e)** Experimentally deformed Magnox alloy containing 0.9% Al and 0.005% Be (30% strain, 200 °C,  $1.9 \times 10^{-4} \text{ s}^{-1}$ ) from Wheeler et al., 2009. Each pixel is coloured by the weighted Burgers vector (WBV) magnitude. The 3D WBV is projected onto the map plane and marked as arrow. **(f)** Naturally deformed Zircon grain BP06/3 from

MacDonald et al., 2013. Each pixel is coloured by a misorientation angle calculated from its orientation relative to a given point.

**4-3** I would be curious to see, for instance, how was measured this subgrain size in the sample deformed at 3% at -10°C, or at 12% at -20°C. I think that the author should clarify this technical aspect as they make a lot of explanation rely on such “average” parameters. Furthermore, provided it is calculated properly, I doubt the distribution is normal, and I think that a metric other than the average would fit best.

The reviewer is correct that the subgrain size distributions are not normal they are skewed in a manner similar to the grain size distributions. In our modification we have tried to focus on elements of the data that are robust and helpful in interpretation. These are basically that subgrains exist and they are smaller than grains. We have removed the data and discussions related to subgrain sizes calculated using boundary misorientation angles of 4°, 6° and 8° (boundary hierarchies) and we have both mean and median subgrain sizes for comparison with grain sizes. The new presentation of data leads to a statement in section 3.3.3: “*Subgrain size distributions (Fig. 4(e), 5(e) and 6(e)) are similar to the grain size distributions (Fig. 4(d), 5(d) and 6(d)), but the median and mean subgrain sizes are smaller than median and mean grain sizes (Table 3).*”

**4-4** In particular, the following assertion is questionable: “because subgrain rotation recrystallization should produce grains that have similar sizes with subgrains, while bulging nucleation should produce grains that have smaller sizes than subgrains” that rely on a parameter (subgrain size) that is ill measured here, since subgrain structure does not resemble at all the one observe in quartz (Halfpenny et al 2012).

We agree with the reviewer that in this case this approach lacks robustness. We removed the extended discussion that including hypotheses of bulging nucleation in the revised manuscript.

**4-5** On top of that, this expected hierarchy of grain size depending from the nucleation mechanism comes from one study on quartz and should not be taken as granted, see for instance Humphreys 2004 (Materials Science Forum) that shows clearly a bulged grain much larger than the surrounding subgrains. It will therefore depend on the material and its anisotropy, and on the resolution of the observations (ability to distinguish between a grain resulting from a bulge and one resulting from subgrain rotation...)

We agree that in this case the boundary hierarchy analyses do not give useful insight and we have removed the hierarchy data and related description and discussion.

**5-1** p8 l. 8-9: To consider  $\langle D_{\text{small}} \rangle$  as a good representative of the mean recrystallized grain size is also a strong hypothesis that should be justified (either by some specific observations or by references from previous work). It will, in particular, depend on the relative effect of grain boundary migration compare to nucleation during recrystallization (and therefore on the temperature of the test) since an apparent small grain size at high GBM rate could well be a 2D cut of a strongly lobated grain, while, at lower temperature (lower GBM rate), small grains indeed are newly recrystallized grains (see for instance the sample deformed at 8% at -10°C, could one certify that small grains observed on the 2D sections are indeed small grains?). Here again appears the necessity of statistic metrics adapted to the observed distributions.

Small grains observed from the EBSD data can be a 2D cross section of a larger 3D grain. We thank the reviewer for these comments as they have pushed us to complete new analyses aiming at quantifying the effects of two distinct (albeit related) stereological issues that add value to this paper and maybe will be useful to others as analytical approaches. The first issue relates to the misidentification of “small” grains, as these could appear from slices cut close to the

perimeter of a large grain in 3-D (Underwood, 1973). The second issue relates to the oversampling of grains that have highly irregular, branching shapes in 3-D and appear more than once on a 2-D surface (Hooke and Hudleston, 1980; Monz et al, 2020). The new analyses are presented in section 3.3.2 (for observation) and 4.1.2 (for discussion). Details of the stereological analyses are presented in section S3 and S4 of the supplementary material. Here we present key findings:

To assess the first issue (misidentification of “small” grains) we extracted one-dimensional grain size measurements (by linear intercept) from two-dimensional maps. From this analysis, we can state whether a “small” 1-D grain is indeed a “small” grain in 2-D. At ~20% strain the percentage of “small” grains on a 1-D line that correspond to “small” grains in the 2-D EBSD map is 64%, 76% and 43% at -30, -20 and -10 °C, respectively. These data suggest that at 20% strain the presence of “small” grains in 3D is likely, with the confidence in this statement increasing at reduced temperatures. Another observation supports this. Figure R1.2 shows examples of “big” and “small” grains in deformed to ~20% strain at -10 °C and -30 °C. Many “small” grains have “small” grain neighbours. At -30 °C some “small” grains are entirely surrounded by other “small” grains. At -10 °C there are lines of “small” grains in contact along the boundary between “large” grains.

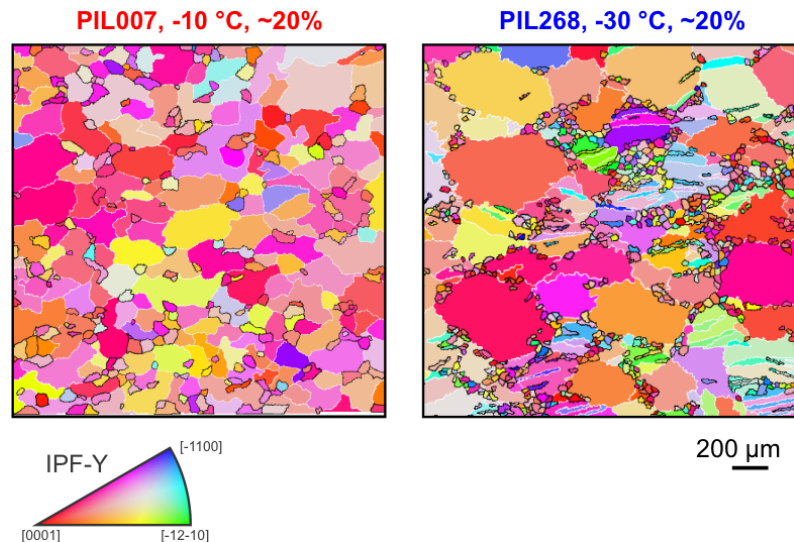


**Figure R1.2.** Examples of “big grains” and “small grains” in PIL007 deformed at -10 °C to ~20% strain, and PIL268 deformed at -30 °C to ~20%. The “small grains” have black grain boundaries, the “big grains” have white grain boundaries. Each grain is coloured by mean orientation with IPF-Y colour code.

It is very difficult (and at -30 C impossible) to have all of these “small” grains linked to large grains in the third dimension whilst maintaining a microstructure that looks like the microstructures in these maps. This is the case at 20% strain. At lower strains the percentage of “small” 1-D segments that correspond to “small” 2-D grains is lower so the confidence with which we can define “small” grains is reduced.

The 1-dimensional data also provide some insight into the second issue, oversampling of grains . In all samples >90% of 2-D grains along an arbitrary line are unique (that is, they are cut only once). Of course, with lines in multiple directions the total percentage of unique grains will decrease. As EBSD provides full crystal orientation data we can extend this analysis to entire maps. We can assess the likelihood of each 2-D mapped grain being connected in the third dimension to another 2-D mapped grain by comparing each grain’s orientation (mean orientation) to all other grains within a certain distance (1mm is used here). If the misorientation between a grain and a nearby grain is below a certain threshold (10°) then we define them as being connected parts of the same grain in 3D. These thresholds probably

overestimate the number of grains connected in 3D. 1mm is more than double the size of the largest grain and  $10^\circ$  is more than twice the median and significantly lower than the upper quartile in mis2mean data (the misorientation angle between all pixels in a grain and the mean orientation of that grain) for all samples. The percentage of “unique” grains (that only appear at the surface once) relative to all grains in a 2D map are higher than 70% at all temperatures and strains (Table S2-S4, Table 3).

The procedure outlined in the last paragraph allows us to estimate the number of “distinct” grains (where all 2-D grains attributed to the same 3-D grain are counted as one grain) in each map and from this, the number density (grain number per unit area) of “distinct” grains. The number density of “distinct” grains increases by more than a factor of 3 relative to the starting material in all samples at all temperatures: reaching values  $> 6$  times initial at  $-10^\circ\text{C}$  and  $>12$  times initial at the lower temperatures. The number density of “distinct” grains is generally higher at strains of  $\epsilon \geq \sim 12\%$  than at strains of  $\epsilon \leq \sim 8\%$  at all temperatures, and it is generally higher in samples deformed at  $-20$  and  $-30^\circ\text{C}$  than samples deformed at  $-10^\circ\text{C}$ .

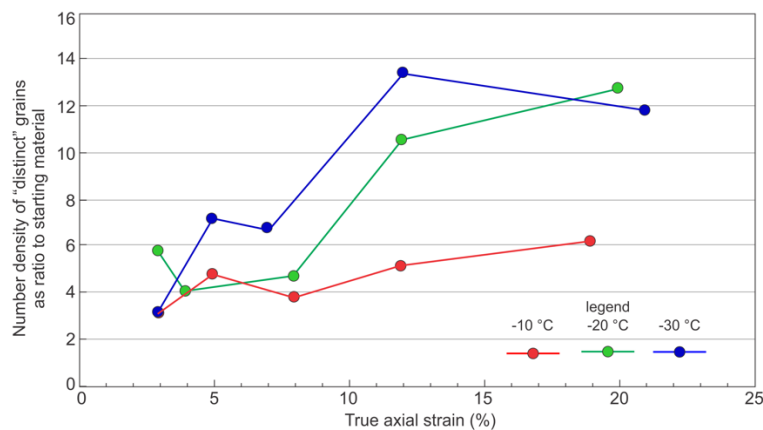


**Figure R1.3.** Number density of “distinct” grains as ratio to starting material relative to true axial strain.

The analyses above provide some confidence that in all the experiments the number density of grains has increased relative to the starting material and increases with strain. That requires new grains to be generated and any measure of average grain size to reduce. If we couple this to the grain size statistics presented and the analysis of whether we are misidentifying small grains, the weight of evidence suggests that we have a real population of smaller grains. Our confidence in this statement increases with reducing temperature and increasing strain.

Having outlined new analyses that add robustness to our statements about reducing grain size with strain and the existence of a population of “small” grains we come back to the issue of how we distinguish “big” and “small” grains. There will always be a degree of arbitrariness in this and to reflect this we added a statement in section 3.3.2: “*Our scheme for separating “big” and “small” grains is not perfect, but it does provide a fast and repeatable way of looking at the possible differences in microstructures and CPO of smaller and larger grains.*”

**5-2** For the sake of clarity, I would suggest the authors not to mix result presentations and interpretations and keep interpretations for the discussion part. In particular when interpretation requires additional hypotheses on top of direct observations and results.

We have been through the manuscript and ensured the observations and interpretations are not mixed up in section 3 (results). We have kept necessary brief descriptions of process in section

3 only for the clarity of concepts introduced from other published works and not for interpretation of our own data.

6. P9 l. 13 “At -10 °C, the CPO intensity of “small grains” is lower than “big grains”, and this contrast becomes strengthened as the temperature decreases.” This could also be related with the fact that it is less straightforward to distinguish small grains from big grains for these tests, this should be mentioned here.

Yes, this is a very good point. The small grain population is easier to define and is better defined at low temperatures than at high temperature. This clearly relates to the differences in the balance of key processes at different temperatures. We hope that we have emphasised this the revised manuscript.

7. P11 l. 26 The authors mention “much of the stress increase prior to peak stress relates to elastic strain”, and, as they notice just after, this is not coherent with the known Young modulus of ice of 9 Gpa... There is a broad literature, dating back to the 70’s and 80’s (Duval et al. 1983, Jacka 1984 for instance, and review by Schulson and Duval 2009) explaining that the transient behavior of ice is not elastic, but anelastic, and is related to the built of an internal stress field related to strain incompatibilities between grains. **I am therefore very astonished to read this sentence here, and I think that this should be corrected before publication.**

The “dissipative deformation” mentioned here is indeed plastic deformation related to intracrystalline dislocation slip, the porosity loss being very likely negligible.

Published literature labelled the stress increase prior to peak stress in constant displacement rate experiments as: “normally elastic” (Cole, 1987) and “quasi-elastic” (Kirby, 1987). The deceleration during primary creep in constant stress experiments was interpreted as effected by a “delayed elasticity”, with a recoverable component of time-dependent elastic strain and an irrecoverable viscous strain (Mellor and Cole, 1982), and “anelasticity” (Duval et al., 1983). The reason we chose to describe the behaviour as substantially elastic is that we have other experiments where we can show that this part of the deformation is recoverable. However, these other experiments are higher rate experiments with slopes on the stress strain curve approaching the 9GPa modulus. The reviewers are correct in pointing out that, in the experiments presented in this paper, the slope is substantially below modulus and the behaviour is not substantially elastic. We have modified the statement in section 4.1.1: “*This likely includes anelastic deformation related to intergranular stress redistribution used to explain primary creep in constant load experiments (Duval et al, 1983). The curvature of the stress strain line at the start of each experiment may relate to initial porosity loss as suggested by rapid increases in ultrasonic p-wave velocity in comparable experiments by Vaughan et al., (2017).*”

**8-1. Part 4.1.1: Discussion about GBS.** The experimental results shown here present no evidence of a grain size sensitive mechanisms, since there is no initial grain size variation, no study of the influence of grain size on the stress – strain-rate relation. I therefore don’t understand why GBS is mentioned here, since it is not necessary at all to explain the observations performed.

Indeed, all results presented here can be explained by intracrystalline dislocation slip accommodated by dynamic recrystallization mechanisms, as very well illustrated in the high quality EBSD observations performed. Furthermore, there exist a large number of studies showing that GBS occurs significantly only in fine-grained materials (see Boullier and Gueguen 1975, Goldsby and Kohlstedt 1997) where grain boundary diffusion can play a role (Ashby 1973). Diffusion in ice is known to be very slow, that renders the hypothesis of a

diffusion-controlled mechanism quite unlikely, especially for large grains, and high strain-rate conditions as encountered here.

The particular set of experiments used in our paper does not include variable initial grain size. However, comparable experiments do show grain size sensitivity. The set of  $-10\text{ }^{\circ}\text{C}$  experiments published by Qi et al 2017 have two different initial grain sizes. A plot of strain rate against the peak stresses (Fig. 3, copied below as Fig. R1.4) shows two different best fit lines for the two initial grain sizes. At peak stress ( $\sim$  equivalent to min strain rate) grain size is unlikely to have changed substantially from the starting material (we have some new experiments to peak stress only that show this to be correct). The easiest interpretation of these data is that there is grain size sensitivity. In this case the sensitivity is manifest between grain sizes of  $\sim 0.25$  (standard ice on Fig. 3 of Qi et al) and  $\sim 0.6\text{mm}$  (course grained ice). There is no clear distinction in the mechanical data for different initial grain sizes at flow stress ( $\sim$ tertiary creep). At flow stress, after strains of  $\sim 0.2$ , grain sizes have evolved substantially and mean grain sizes correlate with the stress magnitude following a piezometer type relationship, as reported for ice by Jacka and Li (1994).

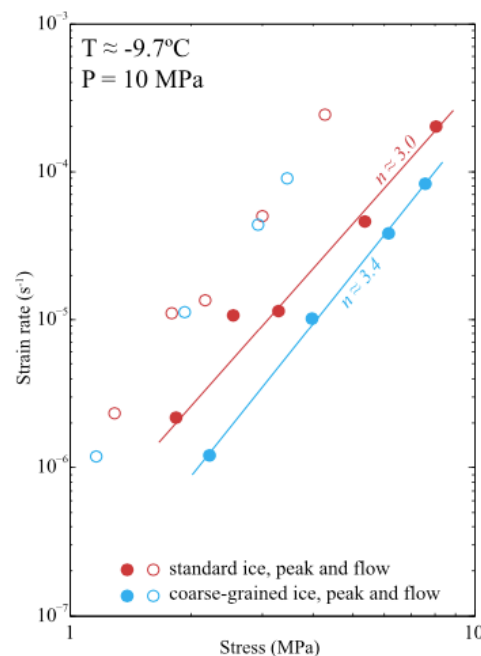


**Figure R1.4.** Plot of strain rate versus stress on logarithmic scales using data from Qi and others (2017).

GBS has always been a problem area since there are few clear microstructural indicators to show that it has occurred: in stark contrast to intracrystalline dislocation slip and accompanying recovery and recrystallisation. Older papers that identify GBS tend to be restricted to studies of very fine materials as it is in these materials that grain size sensitive mechanisms can dominate. An important concept in material science is that mechanisms can co-exist: the whole premise of deformation mechanism maps (<https://engineering.dartmouth.edu/defmech/>) is based on the idea that the total strain rate is the sum of the strain rates related to each contributing deformation mechanism. Recently, Kuiper and others (2019a, 2019b) applied the Goldsby-Kohlstedt composite flow law (which considers bulk strain rate as an additive contribution of dislocation creep and GBS) to model the deformation in NEEM ice core. The extrapolation of the experimental data to natural conditions suggests that “GBS-limited creep produces almost all deformation in the upper 2207 m of depth in the NEEM ice core (grain size between  $\sim 0.3\text{mm}$  and  $\sim 9\text{mm}$ ).” GBS will contribute a larger proportion of total strain rate at

fine grain sizes (e.g. experiments by Goldsby and Kohlstedt (1997)), but can still be significant at coarser sizes.

The advent of EBSD methods has allowed us to analyse microstructures in new ways and to tease out the potential for GBS in a wide range of materials. The change in misorientation axes from rational (along specific crystal directions) to random (w.r.t. crystal directions) with increasing misorientation and the weakening of CPO in recrystallised grains relative to porphyroclasts are two lines of evidence that are commonly used in the rock deformation community (starting with (Bestmann and Prior, 2003; Fliervoet et al., 1999; Jiang et al., 2000) to identify GBS as an operative mechanisms from the analysis of a final microstructure. We realised that we have not presented the basic misorientation analysis (Bestmann and Prior, 2003) and we have now included data on misorientation axes for low angle and high angle boundaries. These data, and the segmentation of CPOs for coarser and finer grains, show the same patterns that are commonly used to infer GBS in deformed rocks. This does not of course prove that GBS has occurred, it merely says that these ice experiments have microstructural characteristics that match other samples where those characteristics have been used to infer GBS.

If GBS does occur, our interpretation is that this is in addition to dislocation glide (Drury et al., 1985; Gifkins, 1976, 1977; Goldsby and Kohlstedt, 1997, 2001; Hirth, 2002; Hirth and Kohlstedt, 2003; Kuiper et al., 2019a; Kuiper et al., 2019b; Langdon, 2006, 2009; Warren and Hirth, 2006). Some authors term this dislocation accommodated GBS or “disGBS”. In this mechanism, the total strain rate is the addition of a dislocation process (that changes crystal shapes and causes lattice rotation and internal distortion) and a GBS process that is probably controlled by a “viscous” mechanism within grain boundaries (small path length diffusion and/or asperity plasticity: idea originally from (Gifkins, 1976)). This is not the same as diffusion creep, irrespective of whether that is controlled by lattice diffusion (Nabarro-Herring creep) or grain boundary diffusion (Coble creep). GBS is required as an accompanying mechanism to polycrystalline diffusion creep, but in that case grain shape change is facilitated by the diffusive mass transfer processes. In diffusion creep, grain size sensitivity comes primarily from the increased path length for diffusion meaning that the change of shape of bigger grains takes longer. In “disGBS” the GBS itself is the prime source of grain size sensitivity. If there is a “viscous” grain boundary volume then the rheology will depend on the volume proportion of the sample that comprises grain boundaries: this proportion will increase with decreasing grain size.

**8-2** The authors could try to calculate the strain-rate expected based on a GBS diffusion flow law (Nabarro-Coble for instance) for similar level of stress as the one of their experiences. They would likely see that the stress – strain-rate curves they obtained are not compatible with a GBS influencing mechanism.

Please see our comments related to diffusion creep in the last paragraph of the response to 8-1.

Also see the response to 15. This outlines how we have modified the discussion of weakening.

Here we expand a little to answer this question: this is from a paper we have in progress to model the effect of grain size on the mechanical evolution of deformed ice and is beyond the scope of inclusion in this paper. The ratio of stress drop after peak is ~35% for samples deformed at warm or cold temperatures (as pointed out elsewhere by the reviewer). A simple model uses just the GBS component of the Goldsby-Kohlstedt composite flow law. The strain rate of GBS can be expressed as:

$$\dot{\epsilon} = A\sigma^n d^{-p} \exp\left(-\frac{Q}{RT}\right), \quad (R1.1)$$

where  $A$  is a material-dependent parameter ( $MPa^{-n}m^p s^{-1}$ ),  $\sigma$  is the stress ( $MPa$ ),  $n$  is the stress exponent,  $d$  is the grain size ( $m$ ),  $p$  is the grain-size exponent,  $Q$  is the activation energy ( $kJmol^{-1}$ ),  $R$  is the gas constant ( $= 8.314 \times 10^{-3} kJmol^{-1}K^{-1}$ ) and  $T$  is the absolute temperature ( $K$ ). The flow law parameters of  $Q$  and  $A$  for GBS ( $n = 1.8, q = 1.4$ ) were taken from Kuiper and others (2019a, 2019b). For each sample, we calculated the stress,  $\sigma$ , by substituting mean or median grain size and temperature (Table 3) into Eq. (R1.1).  $\sigma$  were normalised with respect to the peak stress. Figure R1.5 shows, the normalised stress estimated using the GBS flow law and measured strain rates and grain sizes as a function of strain at both -10 and -30 °C. There is much more work for us to do, but the models give stress strain patterns that have the same general form as the mechanical data, with an underestimate of weakening at -10C and an overestimate at -30 °C.

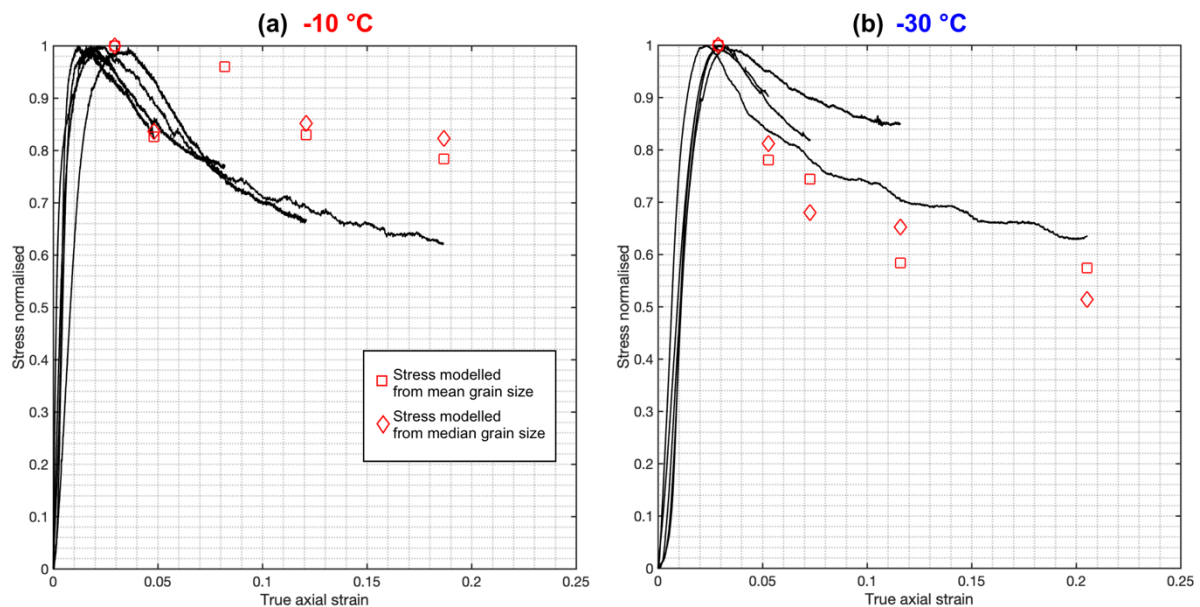


**Figure R1.5.** Normalised stress vs stress for samples deformed at (a) -10 °C and (b) -30 °C. For each temperature series, the stresses estimated from GBS mechanism are normalised by the estimated stress at ~3% strain.

**9 Part 4.1.2:** In this part, the authors use the subgrain size measurements to estimate the role of subgrain rotation in the recrystallization mechanisms.

Once again, the subgrain structure observed here is very far from the ones in quartz, to enable using the paper mentioned here as a reference (Trimby et al. 1998), and I think the authors should be much clearer about the way they evaluate the subgrain size before getting to strong an interpretation from this parameter.

Ice behavior, and in particular in the experiments presented here, is very different from the one of more isotropic materials in the sense that the dislocation substructures are not characterized by subgrain cells as observed in Al or Quartz for instance. This is due to the fact that subgrain substructures as observed in Quartz results from equivalent activity of several slip systems. Although one observe some c-dislocations in the microstructure, slip system activity in ice remains dominated by basal slip, and resulting subgrains have mostly the shape of large tilt and kink bands.

Only close to GB and triple junctions will we find more complex substructures. Is it enough to evaluate an “average” subgrain size? Care must therefore be taken before using interpretations

coming from these more isotropic materials. And explanation should be given about how is this subgrain size measured here.

We agree with the reviewer about the lack of clarity of the measurement of subgrains. We have reduced significantly the discussions related to subgrain size. We have plotted subgrain boundary map based on misorientation angle of neighbouring pixels, added misorientation angle analyses and calculated median subgrain size to better support subgrain analyses. Please refer to responses to comments 4-1 to 4-5 for more details.

**10 P13 l. 1-2:** Indeed, Jacka and Li Jun 1994 evidenced a linear relationship between grain size and stress during dynamic recrystallization of polycrystalline ice (creep experiments, tertiary creep). I think that this should be mentioned here.

We agree with the reviewer. We added a statement in section 4.1.2: “Jacka and Li (1994) show a linear relationship between ice grain size and stress from deformed ice samples that reach tertiary creep.”

**11. P13. l. 5:** here again, caution must be taken with making use of the subgrain size as it is still ill defined... and the ice case can not be compared straightforward to Halpenny et al. studies!

Indeed, observation given l. 16-17 goes in the direction of my remark... Subgrain size, if measurable here, can not be used similarly as in the other studies mentioned since there is no clear subgrain substructure. But, still, subgrain rotation could explain part of the recrystallization by, for instance, closing the bulges (see Chauve et al. 2017, Phil Trans), or by separating grains via highly misoriented tilt or kink bands. But, indeed, one can not talk about “continuous” recrystallization as observed in Al for instance (see Sakai et al. Progress in Materials Science, 60(0):130–207, 3 2014 for a review).

We have modified the manuscript by presenting subgrain structures in a clearer way. Please refer to responses to comments 4-1 to 4-5 for details.

**12. Part 4.1.3 p 14 l. 11:** “Because grains with hard slip orientations should have greater internal distortions”, there is absolutely no proof of that in ice, and some recent work tend to show that there is no systematic relation between orientation and strain localisation (see Grennerat et al. 2012 for instance) or between orientation and subgrains density (see Journaux et al. 2019 for instance). I think it should not be considered as granted, in particular when not shown directly in your experiments. Have you tried, for instance, to measure the density of GNDs as a function of grain orientation?

We modified our statement in 4.1.3 to: “*Cone-shaped c-axes CPOs have been related to strain-induced GBM favouring the growth of grains with easy slip orientations (high Schmid Factors) (Duval and Castelnau., 1995; Little et al., 2015; Vaughan et al., 2017; Qi et al., 2017). Linked to this is the idea that grains with hard slip orientations should have greater internal distortions (Duval and Castelnau., 1995; Bestmann and Prior 2003), and therefore store higher internal strain energy. If this is correct then hard slip grains are likely to be consumed by grains with easy slip orientations through GBM (Duval and Castelnau., 1995; Piazzolo et al., 2006; Killian et al., 2011; Qi et al., 2017; Xia et al., 2018). However, we have to re-evaluate the detail of this idea, as recent studies on deformed ice samples show there is no systematic relation between orientation and strain localisation at low strain (Grennerat et al. 2012). Furthermore, studies of high-strain shear samples find no clear difference in the geometrically necessary dislocation density within the two maxima that develop in simple shear (Journaux et al. 2019). An alternative, and as yet incomplete, explanation from Kamb (1959) relates recrystallisation directly to the elastic anisotropy of crystals and through this to the orientation of the stress field. At this stage the observation that ice CPOs developed at relatively high temperature and particularly at low strain correspond to high Schmid factor*

orientations remains robust. The underlying mechanisms will need continual review as we collect new data.”

We have done a whole series of quantitative Weighted Burgers vector (WBV) analyses on our EBSD data. However, we decided to pull all the WBV analyses out from this paper because we found a strong stereological effect, i.e. effects of different 2-D surfaces chosen from the same 3-D sample, on the GND statistics. We will present unpublished data only for discussion here. These data are subject for future publication. We conducted pixel-by-pixel WBV analyses on different orthogonal surfaces from the same deformed ice samples.

An analysis of a uniaxially deformed sample with a nearly random overall CPO (PIL165: 3% strain) illustrates the problem (Fig. R1.6). The absolute values of WBV and the relative values of WBV for grains in different orientations change depending upon which surface (normal or parallel to shortening) is being examined by EBSD.

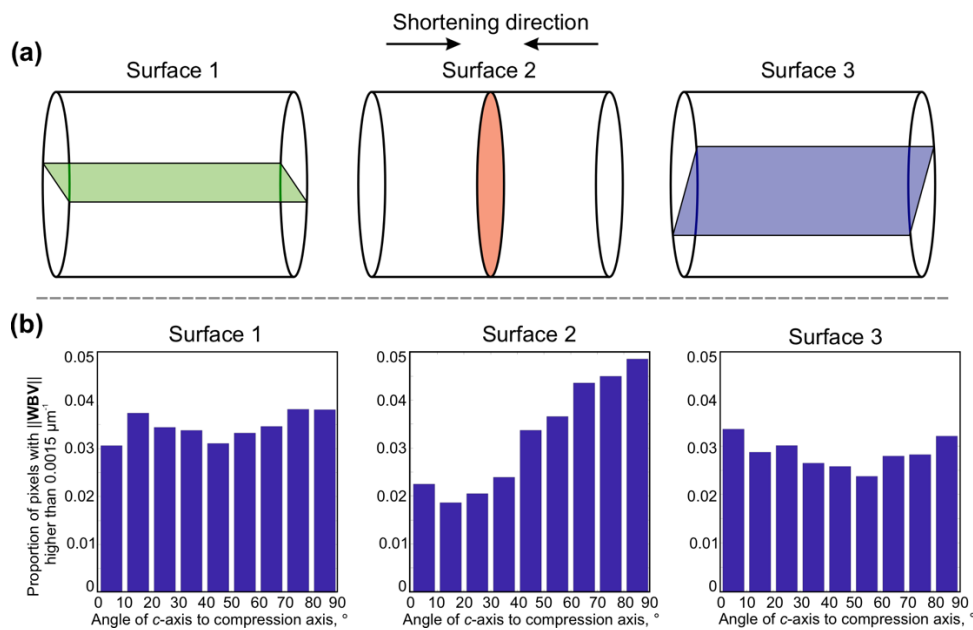


**Figure R1.6.** (a) Illustration of three orthogonal surfaces chosen from a sample (PIL165,  $-30\text{ }^{\circ}\text{C}$ ,  $\sim 3\%$  strain,  $1 \times 10^{-5}\text{ s}^{-1}$ ) for WBV analyses. (b) Proportion of pixels with the magnitude of WBV ( $\|\mathbf{WBV}\|$ ) higher than  $0.0015 \mu\text{m}^{-1}$  as a function of  $c$ -axis angle to compression axis.

In uniaxially compressed and sheared samples, with strong CPOs, the WBV of different texture components depend on the orientation of the sample surface analysed (Figure R1.7). The WBV of the of the distinct  $c$ -axis maxima ( $\sim 45$  degrees to compression and normal to shear plane respectively) depend on the orientation of the surface examined (Table R1.1).

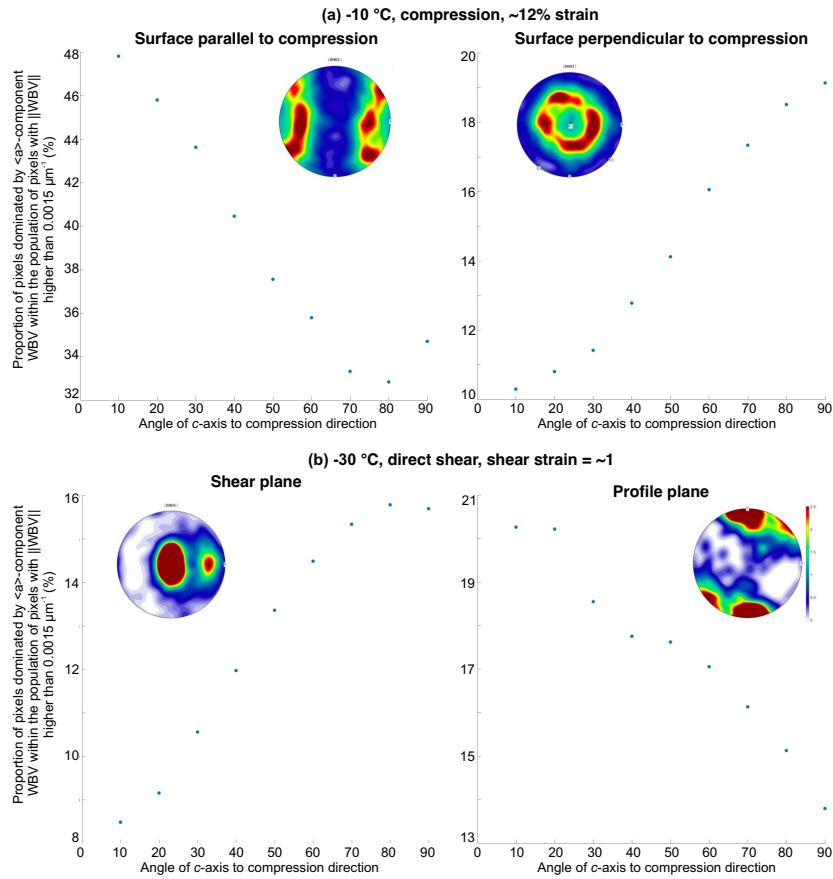


**Figure R1.7.** Differences between planes parallel or perpendicular to compression or shear in the proportion of basal-component pixels with  $\|\mathbf{WBV}\|$  higher than  $0.0015 \mu\text{m}^{-1}$  as a function of  $c$ -axis angle to compression for **(a)** PIL177, sample deformed with uniaxial compression at  $-10 \text{ }^\circ\text{C}$  to  $\sim 12\%$  strain with a strain rate of  $1 \times 10^{-5} \text{ s}^{-1}$ , and **(b)** PIL267, sample deformed with direct shear at  $-30 \text{ }^\circ\text{C}$  to a shear strain of  $\sim 1$  with a shear strain rate of  $\sim 1.8 \times 10^{-5} \text{ s}^{-1}$ .

**Table R1.1.** WBV statistics of grains at easy slip orientations from orthogonal surfaces

Sample No.	Surface type	$c$ -axis orientations included in analysis	Proportion of pixels with the magnitude of WBV ( $\ \mathbf{WBV}\ $ ) higher than $0.0015 \mu\text{m}^{-1}$	Proportion of pixels dominated by <a>-component WBV within the population of pixels with $\ \mathbf{WBV}\ $ higher than $0.0015 \mu\text{m}^{-1}$
PIL177	Parallel to compression	$45^\circ \pm 5^\circ$ to compression axis	9%	42%
	Perpendicular to compression		3%	31%
PIL267	Shear plane	$0^\circ$ - $30^\circ$ to compression axis	10%	25%
	Profile plane		26%	51%

The statistics of WBV data are different when the same sample is looked at using different imaging surfaces. (e.g. shear plane vs profile plane). A running hypothesis is that the dislocations are mostly arranged in planar subgrain boundaries and the frequency of observation depends on the orientation of the grain relative to the observation surface. The orientation of the subgrain boundary is a function of grain orientation and Burgers vector. Stereological effects need to be taken special care of when quantifying GNDs from the EBSD

data acquired from a single 2-D sample surface. Conclusions derived from GND calculations can be strongly biased by different imaging surfaces. It is not straightforward to compare different texture components where the relative orientation of c-axes and imaging surface are different. Note that the data and conclusions in (Journaux et al., 2019) will probably not be compromised by this effect as, in the profile plane in which the samples were analysed, the M1 and M2 maxima have identical relative orientations of c-axis and analysis surface.

### 13. P14 l. 20: GBM instead of GMB

This mistake has been corrected.

**14-1.** About GBS and apparent texture weakening in small grains: to my point of view, this apparent texture weakening could be related to the nucleation process itself, and the fact that close to GBs, local misorientation can be high, and induce nucleation orientations varying from parent grains orientations (by bulging or subgrain rotation). This process would be enough to justify the small difference in texture concentration in small grains (that could also be due to more spread in data as there are less pixels measured in small grains, since GBs are interfering with the measurement, reducing its quality in small grain areas?). See for instance the work of Falus et al. 2011 about Olivine for rotation recrystallization or Chauve et al. 2017 for the orientation of nucleus formed by bulging.

If “spontaneous” nucleation, driven by the relaxation of the dislocation-related internal stress field, can produce nuclei with orientations not related to their corresponding parent grains (Duval et al., 2012), we agree that this could lead to a weaker CPO. For this reason, we have included this as an alternative explanation to the GBS idea.

We added new statements in section 4.1.4: “ “*Spontaneous*” nucleation driven (Duval et al 2012) by the relaxation of the dislocation-related internal stress field may produce nuclei with orientations not related to their corresponding parent grains (Falus et al., 2011; Chauve et al., 2017), and thus lead to a weaker CPO.’... ‘Both hypotheses— “spontaneous” nucleation and GBS—explain a weakening of CPO in “small” grains and these two ideas are not mutually exclusive. Further work is needed to test both hypotheses. Most critical are experiments where nuclei can be observed whilst they are very small and subsequent misorientations can be documented, as might be possible with 3-D microscopy methods (Lauridsen et al, 2003; Poulson et al., 2004), and experiments where fiducial markers are used to confirm the physical existence of offsets on grain boundaries (Schmid et al, 1977; Spiers 1979 ; Beeré, 1978; Eleti et al., 2020).’ ”

The data in Chauve et al (2017) can be interpreted equally well by GBS as by spontaneous nucleation and bulging, as was pointed out by the reviewer (Prior) of that paper. Falus et al is one of the few papers in the geoscience world that interprets weakening CPO with reduced grain size as related to a spontaneous nucleation process. There are many more papers (excluding our papers) (Cao et al., 2017; Czertowicz et al., 2016; Kaczmarek and Tommasi, 2011; Linckens et al., 2015; Ohuchi et al., 2015; Park and Jung, 2017; Skemer and Karato, 2008; Skemer et al., 2010; Warren and Hirth, 2006; Warren et al., 2008; Zhao et al., 2019) that interpret almost identical data in terms of the operation of GBS. We think the best way forward in our paper is to make sure that the factual observations are clear and to present both ways (GBS and spontaneous nucleation) that have been used in the literature to interpret similar data.

We don’t think that the measurement of fewer pixels in the smaller grains makes any contribution to the weaker CPOs identified. The CPOs are weaker irrespective of whether all pixels are used or one point per grain. They are weaker if we choose a random subset of grains so that the number of “big” and “small” grains are the same.

**14-2** The work of Qi et al. 2017 mentioned several times in this part concluded that “the dominant mechanism of CPO development occurs with increasing stress, from GBM, which consumes grains with low Schmid factors, at low stress, to the rotation of basal slip planes to an orientation normal to the compression axis at high stress, due to dislocation glide.” I didn’t find any mention of “grain size sensitive mechanism” as certified l. 25...

Such a grain size sensitive mechanism should be verified by varying grain size during the experiments and evaluate its effect on a given parameter, such as peak stress, strain-rate or so. I maintain that there is no proof of such a GSS mechanism in the experiments presented here, and therefore the interpretation should be cleared about that. That GBS is more active in smaller grains is well known since Boullier and Gueguen work! It does not mean that it should occur in the specific case here, unless otherwise proven...

We agree that rotation of slip planes is a key process in CPO evolution and hopefully our revisions make that much clearer. If GBS occurs it is additional to lattice rotations related to dislocation activity. In the work referred to (Qi et al., 2017: that involves three of the co-authors of this paper) we did not segment the data in a way that required us to bring in interpretations such as GBS, nor spontaneous nucleation. We were always of the view that GBS could be important, as that paper does show the grain size sensitivity of peak stress data. However, it was really the work published by (Craw et al., 2018) that highlighted for the first time an extreme (in that case) difference between CPOs at different grain sizes. GBS is an integral part of the interpretation in that paper and was included in (Qi et al., 2019) to explain some of the features of shear CPOs that are not easily explained by basal slip or dynamic recrystallisation.

**14-3** The hypothesis that GBM being less active at low temperature, the impact of grain rotation driven by intracrystalline slip prevails is much clearer, especially since it is very coherent with the observations that the cone angle is reduced, and more orientations are found close to the vertical. This assertion is, indeed, justified by the experimental observations. This is, in fact, the main “novelty” of the presented work and should be emphasised more. Speculation about GBS tends to lessen this message, and also the interest of the good quality observations performed in this work.

We agree with this and hopefully the revised manuscript makes this clear.

**15** During dynamic recrystallization, weakening is classically (see Humphreys and Haterly 2001 or 2004 for instance, Sakai et al. 2014) attributed to the reduction of hardening based on GBM and nucleation of grains, both reducing the stored strain energy associated with dislocation pile-up or dislocation structures. Therefore dynamic recrystallization induced weakening does not require the interplay of CPO or grain-size sensitive mechanism to be explained. Another point for this consideration about weakening: the relative weakening at about 20% strain is similar for every temperature cases, at about 35% ( $\sigma_p - \sigma_f / \sigma_p$ ). Therefore there is not more weakening with small grains than without... It should rule out the hypothesis of a grainsensitive mechanism to explain weakening. Nucleation and GBM (each one having different relative influence depending on the temperature) are enough to explain the observed weakening, as expected from the dynamic recrystallization literature.

We agree with the reviewer that balance between GBM and nucleation can also explain the mechanical weakening and it is important to add this into the discussion. One key issue we want to be clear about is that CPO development is not necessarily the key process controlling weakening (or enhancement): an idea that seems prevalent among the ice sheet modelling community. We modified the statements in section 4.2: “ *All experiments show weakening after peak stress. Weakening is classically observed during dynamic recrystallization, and it*

has been attributed to a balance between GBM and nucleation of new grains (Montagnat and Duval., 2000; Sakai et al., 2014). In this study, mean and median ice grain size reduces with strain at all temperatures (Table 3, Fig. 11(a)). Grain size is commonly reduced during rock deformation in the laboratory (e.g. Pieri et al., 2001; Hansen et al., 2012) and in nature (Trimby et al., 1998; Bestmann and Prior, 2003). At smaller grain sizes the strain rate contribution of grain size sensitive (GSS) mechanisms increases or the stress required to drive a given strain rate contribution of GSS decreases. '... 'Therefore, further studies are required to quantify: (1) the contribution of nucleation and GBM to the total stress drop if the balance of GBM and nucleation is considered as the weakening mechanism; (2) The contribution of grain size insensitive, e.g. dislocation creep, and grain size sensitive processes, e.g. GBS, to the total stress drop if grain size reduction is considered as the weakening mechanism.' "

**16 Point 2:** from figure 2, the steady state is not so obviously reached, unless, maybe at -10°C. Maybe the authors should be more careful about it, especially about mentioning it in the conclusion.

We have modified the statement to: "In all samples stress rises to a peak stress at ~ 1 to 4% strain and then drops to lower stresses at higher strains."

**17 Point 3:** regarding my previous comments concerning the evaluation of a subgrain size, I think that either the authors explain very clearly how they evaluate this subgrain size, and show that it is meaningful based on their experimental observations (that they do observe a subgrain network, although it does not appear clearly in the given figures, from which extracting a subgrain size appears relevant), or this parameter, even if used in the discussion with care, should not appear in the conclusion.

We removed WBV analyses. Instead, we added subgrain boundary analyses by highlighting subgrain boundaries at where the misorientations between neighbouring pixels are between 2° and 10° (Fig. 4(a-c), 5(a-c) and 6(a-c) in modified manuscript). Many of the subgrain boundaries appear to be straight, with some variations around the straight shape. The subgrain boundaries close to bulged grain boundaries are more curved. An interconnection of subgrain boundaries can be observed in some of the grains.

We didn't make it clear that the measurement of subgrain sizes were not based on the data of WBV, and they were based on the misorientation between adjacent pixels. Therefore, the new subgrain boundary plots corresponds to the original subgrain calculations.

We modified the point 3 to: "*All deformed samples develop distinct subgrain boundaries and show a peak at 2°-3° in neighbour-pair misorientation angle distribution. Mean/median subgrain size is smaller than mean/median grain size. These observations suggest recovery and subgrain rotation were active in all deformed samples.*"

**18 Point 5:** once again, this conclusion makes use of the subgrain size which measurement method is not clear, and therefore should not be used in the conclusion unless clarified.

We have removed this conclusion since description and discussion of subgrain size have been strongly reduced.

**19 Point 6:** I think that there is nothing really new in this point... it has been demonstrated for many materials undergoing dynamic recrystallization, and it is a direct evidence from energy considerations... Should it really come as an important conclusion? At least, the authors should be care to mentioned "as already observed", or "as expected during dynamic recrystallization"...

We have removed boundary lobateness analyses. This is an issue for a different readership.

**20** Point 7: based on my comments concerning part 4.2, the mention of GBS to explain weakening should be removed. It is also surprising that an hypothesis that is only briefly mentioned in a very short paragraph (4.2), could come to an important conclusion point...

See responses to 8-1, 8-2 and 14-2.

**21** Point 8: same as point 7, and please note that weakening should be measured relatively to the peak stress value (for instance), and it therefore leads to very similar weakening for all temperature conditions (about 35%).

We have removed point 8.

**21** - In general, there is a lack of references from the work done on recrystallization (on ice and other materials) by others authors than the authors' team.... this is especially true, for instance, in part 4.1.3, and this should be corrected. In particular when other's work do not come to similar conclusions as the authors...

We have included additional references in the modified manuscript.

**22.** - Maybe related to this lack of references, some assertions are given with too few justifications, that should come either from experimental observations or from previous works. This should be corrected, and the authors could specify that they are making hypotheses when there is no existing justifications.

We have added more references on concepts that are not clarified. We have specified that we are making hypotheses or interpretations wherever that is the case.

**23** - This work does not contain any significant novelty, but provides more detailed and accurate observations at the microstructure scale compared to previous (old!) measurements performed by Jacka and co-authors for instance.

Compared to the extensive literature about dynamic recrystallization at hot temperature (see for instance Humphreys and Haterly 2001 or 2004), there is no novelty, and this literature should be mentioned, especially within the discussion, in order to help the interpretation of the results.

This paper include quantitative microstructural analysis of ice deformed at -20 and -30 °C to progressively higher strains. Such data have never been presented before. To our point of view, these new data are novel. See the comments in section one (General statements)

We present the opening angle evolution of the cone-shaped *c*-axis CPO between this study and previous work. This work had not been systematically done before. The summary view of observations of open-angle evolution with strain as a function of temperature (and ultimately also as a function of stress/ strain rate) is crucial as a test of hypothesis for the deformation and recrystallisation mechanisms that control ice microstructure and ice mechanics.

Last but not the least, we added more data, including misorientation analyses and quantification of repeat counted grains in 2-D using line interception method (done before) and full crystallographic data (completely new) to provide a more detailed microstructural analyses, and to support hypotheses.

**24** - The high quality observations enable to assert more clearly some mechanisms as important in the case of recrystallization in ice as, for instance, the fact that at low temperature, intracrystalline rotation will prevail on GBM and therefore induces texture that are closer to the one observed along deep ice cores.

We agree with the reviewer on this point. We hope we have done this in the modified manuscript.

25 - It is not clear, all over the text, why the authors want or need to mention GBS as an impacting mechanism since the experiments performed show absolutely no proof of it, neither in macroscopic data (dependence of peak stress on grain size for instance), nor in microscopic observations. The only observation of small grain necklaces (but limited in number) at the lowest temperature, and a weaker texture in this small grain population is not sufficient, to my point of view, to assert the occurrence of GBS. It could be mentioned as one of the hypothesis among others, but not come to the conclusion as the mechanism at play. In particular, the use of GBS is not necessary to explain stress weakening and does not appear coherent with the results.

See responses to 8-1, 8-2 and 14-2.

26 - I raise again the point about the lack of proper explanation concerning the measurement of subgrain size in the specific case the presented experiments, since the figures shown do not reveal any proper subgrain structure that could be characterized by a dimension (as a mean size for instance). Since different conclusion are taken out of this subgrain size evaluation, it should be corrected before any publication.

We agree with the reviewer. We have provided new subgrain boundary maps and new subgrain/grain size data. We also strongly reduced data and discussion related to subgrain size.

27 - the authors make no use of their observations from the WBV method neither in the discussion, nor in the conclusion... Should it remain in the paper?

We have removed WBV analyses. We have done a whole series of quantitative Weighted Burgers vector (WBV) analyses on our EBSD data. However, we decided to pull all the WBV analyses out from this paper because we found a strong stereological effect, i.e. effects of different 2-D surfaces chosen from the same 3-D sample, on the GND statistics. Please refer to response to comment 12 for details.

## References

Becroft, L., 2015, New grain growth experiments in water ice [MSc thesis: University of Otago, p132].

Bestmann, M. and Prior, D. J.: Intragranular dynamic recrystallization in naturally deformed calcite marble: diffusion accommodated grain boundary sliding as a result of subgrain rotation recrystallization, *Journal of Structural Geology*, 25(10), 1597–1613, [https://doi.org/10.1016/s0191-8141\(03\)00006-3](https://doi.org/10.1016/s0191-8141(03)00006-3), 2003.

Cao, Y., Jung, H. and Song, S.: Olivine fabrics and tectonic evolution of fore-arc mantles: A natural perspective from the Songshugou dunite and harzburgite in the Qinling orogenic belt, central China, *Geochem. Geophys. Geosyst.*, 18(3), 907–934, <https://doi.org/10.1002/2016GC006614>, 2017.

Chauve, T., Montagnat, M., Barou, F., Hidas, K., Tommasi, A. and Mainprice, D.: Investigation of nucleation processes during dynamic recrystallization of ice using cryo-EBSD, *Phil. Trans. R. Soc. A*, 375(2086), 20150345–20, <https://doi.org/10.1098/rsta.2015.0345>, 2017.

Cole, D. M.: Strain-Rate and Grain-Size Effects in Ice, *Journal of Glaciology*, 33(115), 274–280, <https://doi.org/10.3189/S0022143000008844>, 1987.

Craw, L., Qi, C., Prior, D. J., Goldsby, D. L. and Kim, D.: Mechanics and microstructure of deformed natural anisotropic ice, *Journal of Structural Geology*, 115, 152–166, <https://doi.org/10.1016/j.jsg.2018.07.014>, 2018.

Cross, A. J., Prior, D. J., Stipp, M. and Kidder, S.: The recrystallized grain size piezometer for quartz: An EBSD-based calibration, *Geophysical Research Letters*, 44, 6667–6674, <https://doi.org/10.1002/2017gl073836>, 2017a.

Czertowicz, T. A., Toy, V. G. and Scott, J. M.: Recrystallisation, phase mixing and strain localisation in peridotite during rapid extrusion of sub-arc mantle lithosphere, *Journal of Structural Geology*, 88(c), 1–19, <https://doi.org/10.1016/j.jsg.2016.04.011>, 2016.

Duval, P., Ashby, M. F. and Anderman, I.: Rate-controlling processes in the creep of polycrystalline ice, *The Journal of Physical Chemistry*, 87(21), 4066–4074, <https://doi.org/10.1021/j100244a014>, 1983.

Duval, P., Louchet, F., Weiss, J. and Montagnat, M.: On the role of long-range internal stresses on grain nucleation during dynamic discontinuous recrystallization, *Materials Science & Engineering A*, 546, 207–211, <https://doi.org/10.1016/j.msea.2012.03.052>, 2012.

Fliervoet, T. F., Drury, M. R., & Chopra, P. N: Crystallographic preferred orientations and misorientations in some olivine rocks deformed by diffusion or dislocation creep. *Tectonophysics*, 303, 1–27. [https://doi.org/10.1016/s0040-1951\(98\)00250-9](https://doi.org/10.1016/s0040-1951(98)00250-9), 1999.

Goldsby, D. L. and Kohlstedt, D. L.: Grain boundary sliding in fine-grained ice I, *Scripta Materialia*, 37, 1399–1406, [https://doi.org/10.1016/s1359-6462\(97\)00246-7](https://doi.org/10.1016/s1359-6462(97)00246-7), 1997.

Hansen, L. N., Zimmerman, M. E., and Kohlstedt, D. L.: The influence of microstructure on deformation of olivine in the grain-boundary sliding regime, *J. Geophys. Res.*, 117, B09201, <https://doi.org/10.1029/2012JB009305>, 2012.

Hidas, K., Tommasi, A., Mainprice, D., Chauve, T., Barou, F. and Montagnat, M.: Microstructural evolution during thermal annealing of ice-Ih, *Journal of Structural Geology*, 99, 31–44, <https://doi.org/10.1016/j.jsg.2017.05.001>, 2017.

Hooke, R. L. and Hudleston, P. J.: Ice Fabrics in a Vertical Flow Plane, Barnes Ice Cap, Canada, *Journal of Glaciology*, 25(92), 195–214, <https://doi:10.3189/S0022143000010443>, 1980.

Humphreys, J. F.: Nucleation in Recrystallization, *MSF*, 467–470, 107–116, <https://doi.org/10.4028/www.scientific.net/msf.467-470.107>, 2004.

Jiang, Z., Prior, D. J. and Wheeler, J.: Albite crystallographic preferred orientation and grain misorientation distribution in a low-grade mylonite: implications for granular flow, *Journal of Structural Geology*, 22(11-12), 1663–1674, [https://doi.org/10.1016/s0191-8141\(00\)00079-1](https://doi.org/10.1016/s0191-8141(00)00079-1), 2000.

Journaux, B., Chauve, T., Montagnat, M., Tommasi, A., Barou, F., Mainprice, D. and Gest, L.: Recrystallization processes, microstructure and crystallographic preferred orientation evolution in polycrystalline ice during high-temperature simple shear, *The Cryosphere*, 13(5), 1495–1511, <https://doi.org/10.5194/tc-13-1495-2019>, 2019.

Kaczmarek, M.-A. and Tommasi, A.: Anatomy of an extensional shear zone in the mantle, Lanzo massif, Italy, *Geochem. Geophys. Geosyst.*, 12(8), 1–24, <https://doi.org/10.1029/2011GC003627>, 2011.

Kilian, R., Heilbronner, R., and Stünitz, H.: Quartz grain size reduction in a granitoid rock and the transition from dislocation to diffusion creep, *Journal of Structural Geology*, 33, 1265–1284, <https://doi.org/10.1016/j.jsg.2011.05.004>, 2011.

Kirby, S. H., Durham, W. B., Beeman, M. L., Heard, H. C. and Daley, M. A.: Inelastic properties of ice Ih at low temperatures and high pressures, *J. Phys. Colloques*, 48(C1), C1–227–C1–232, <https://doi.org/10.1051/jphyscol:1987131>, 1987.

Kuiper, E. J. N., Weikusat, I., de Bresser, J. H., Jansen, D., Pennock, G. M., and Drury, M. R.: Using a composite flow law to model deformation in the NEEM deep ice core, Greenland: Part 1 the role of grain size and grain size distribution on the deformation of Holocene and glacial ice, *The Cryosphere Discuss*, <https://doi.org/10.5194/tc-2018-275>, 2019a.

Kuiper, E. J. N., de Bresser, J. H. P., Drury, M. R., Eichler, J., Pennock, G. M. and Weikusat, I.: Using a composite flow law to model deformation in the NEEM deep ice core, Greenland: Part 2 the role of grain size and premelting on ice deformation at high homologous temperature, *The Cryosphere Discussions*, <https://doi.org/10.5194/tc-2018-275>, 2019b.

Linckens, J., Herwegh, M., & Müntener, O: Small quantity but large effect — How minor phases control strain localization in upper mantle shear zones. *Tectonophysics*, 643, 26–43. <https://doi.org/10.1016/j.tecto.2014.12.008>, 2015.

MacDonald, J. M., Wheeler, J., Harley, S. L., Mariani, E., Goodenough, K. M., Crowley, Q. and Tatham, D.: Lattice distortion in a zircon population and its effects on trace element mobility and U–Th–Pb isotope systematics: examples from the Lewisian Gneiss Complex, northwest Scotland, *Contrib Mineral Petrol*, 166, 21–41, <https://doi.org/10.1007/s00410-013-0863-8>, 2013.

Mellor, M. and Cole, D. M.: Deformation and failure of ice under constant stress or constant strain-rate, *Cold Regions Science and Technology*, 5(3), 201–219, [https://doi.org/10.1016/0165-232x\(82\)90015-5](https://doi.org/10.1016/0165-232x(82)90015-5), 1982.

Monz, M. E., Hudleston, P. J., Prior, D. J., Michels, Z., Fan, S., Negrini, M., and Langhorne, P.: Electron backscatter diffraction (EBSD) based determination of crystallographic preferred orientation (CPO) in warm, coarse-grained ice: a case study, Stornglaciären, Sweden, *The Cryosphere Discuss*, <https://doi.org/10.5194/tc-2020-135>, 2020.

Ohuchi, T., Kawazoe, T., Higo, Y., Funakoshi, K.-I., Suzuki, A., Kikegawa, T. and Irifune, T.: Dislocation-accommodated grain boundary sliding as the major deformation mechanism of olivine in the Earth's upper mantle, *Sci. Adv.*, 1(9), e1500360–11, <https://doi.org/10.1126/sciadv.1500360>, 2015.

Park, M., and Jung, H: Microstructural evolution of the Yugu peridotites in the Gyeonggi Massif, Korea: Implications for olivine fabric transition in mantle shear zones. *Tectonophysics*, 709, 55–68. <https://doi.org/10.1016/j.tecto.2017.04.017>, 2017.

Prior, D. J., Diebold, S., Obbard, R., Daghlian, C., Goldsby, D. L., Durham, W. B. and Baker, I.: Insight into the phase transformations between ice Ih and ice II from electron backscatter diffraction data, *Scripta Materialia*, 66(2), 69–72, <https://doi.org/10.1016/j.scriptamat.2011.09.044>, 2012.

Prior, D. J., Diebold, S., Obbard, R., Daghlian, C., Goldsby, D. L., Durham, W. B. and Baker, I.: Insight into the phase transformations between ice Ih and ice II from electron backscatter diffraction data, *Scripta Materialia*, 66(2), 69–72, <https://doi.org/10.1016/j.scriptamat.2011.09.044>, 2012.

Qi, C., Goldsby, D. L. and Prior, D. J.: The down-stress transition from cluster to cone fabrics in experimentally deformed ice, *Earth and Planetary Science Letters*, 471, 136–147, <https://doi.org/10.1016/j.epsl.2017.05.008>, 2017.

Qi, C., Prior, D. J., Craw, L., Fan, S., Llorens, M.-G., Griera, A., Negrini, M., Bons, P. D. and Goldsby, D. L.: Crystallographic preferred orientations of ice deformed in direct-shear experiments at low temperatures, *The Cryosphere*, 13(1), 351–371, <https://doi.org/10.5194/tc-2018-140-ac2>, 2019.

Seidemann, M., 2017, Microstructural evolution of polycrystalline ice during non-steady state creep [PhD thesis: University of Otago, p110].

Shigematsu, N., Prior, D. J. and Wheeler, J.: First combined electron backscatter diffraction and transmission electron microscopy study of grain boundary structure of deformed quartzite, *Journal of Microscopy*, 224(3), 306–321, <https://doi.org/10.1111/j.1365-2818.2006.01697.x>, 2006.

Skemer, P. and Karato, S.-I.: Sheared Iherzolite xenoliths revisited, *Journal of Geophysical Research*, 113(B7), 469–14, <https://doi.org/10.1029/2007JB005286>, 2008.

Skemer, P., Warren, J. M., Kelemen, P. B. and Hirth, G.: Microstructural and Rheological Evolution of a Mantle Shear Zone, *Journal of Petrology*, 51(1-2), 43–53, <https://doi.org/10.1093/petrology/egp057>, 2010.

Underwood, E. E., Quantitative Stereology for Microstructural Analysis, in McCall, J. L., and Mueller, W. M., eds., *Microstructural Analysis: Tools and Techniques*: Boston, MA, Springer US, p. 35-66, 1973.

Warren, J. M. and Hirth, G.: Grain size sensitive deformation mechanisms in naturally deformed peridotites, *Earth and Planetary Science Letters*, 248(1-2), 438–450, <https://doi.org/10.1016/j.epsl.2006.06.006>, 2006.

Warren, J. M., Hirth, G. and Kelemen, P. B.: Evolution of olivine lattice preferred orientation during simple shear in the mantle, *Earth and Planetary Science Letters*, 272(3-4), 501–512, <https://doi.org/10.1016/j.epsl.2008.03.063>, 2008.

Wheeler, J., Mariani, E., Piazzolo, S., Prior, D. J., Trimby, P., and Drury, M. R.: The weighted Burgers vector: a new quantity for constraining dislocation densities and types using electron backscatter diffraction on 2-D sections through crystalline materials, *Journal of microscopy*, 233, 482-494, <https://doi.org/10.1111/j.1365-2818.2009.03136.x>, 2009.

Zhao, N., Hirth, G., Cooper, R. F., Kruckenberg, S. C. and Cukjati, J.: Low viscosity of mantle rocks linked to phase boundary sliding, *Earth and Planetary Science Letters*, 517, 83–94, <https://doi.org/10.1016/j.epsl.2019.04.019>, 2019.